Effects of Heme on the Structure of the Denatured State and Folding Kinetics of Cytochrome b562

ARTICLE *in* JOURNAL OF MOLECULAR BIOLOGY · MARCH 2005

Impact Factor: 4.33 · DOI: 10.1016/j.jmb.2004.11.044 · Source: PubMed

11 AUTHORS, INCLUDING:

Marta Bruix
Spanish National Research Council
178 PUBLICATIONS **3,457** CITATIONS
SEE PROFILE

Simone Ciofi
University of Florence
71 PUBLICATIONS **2,701** CITATIONS
SEE PROFILE

Heinrich Roder
Fox Chase Cancer Center
121 PUBLICATIONS **8,472** CITATIONS
SEE PROFILE

Alan Fersht
University of Cambridge
629 PUBLICATIONS **52,768** CITATIONS
SEE PROFILE

doi:10.1016/j.jmb.2004.11.044 J. Mol. Biol. (2005) 346, 331–344

JMB

Available online at www.sciencedirect.com

SCIENCE DIRECT®

ELSEVIER

Effects of Heme on the Structure of the Denatured State and Folding Kinetics of Cytochrome b_{562}

Pascal Garcia[1], Marta Bruix[1], Manuel Rico[1], Simone Ciofi-Baffoni[2] Lucia Banci[2], M. C. Ramachandra Shastry[3], Heinrich Roder[3] Thierry de Lumley Woodyear[4], Christopher M. Johnson[4], Alan R. Fersht[4] and Paul. D. Barker[4]*

[1]*Instituto de Química Física Rocasolano, CSIC, C/Serrano 119, 28006 Madrid, Spain*

[2]*Department of Chemistry and Magnetic Resonance Center CERM, University of Florence Via Luigi Sacconi 6, 50019 Sesto Fiorentino, Florence Italy*

[3]*Fox Chase Cancer Center Institute for Cancer Research Philadelphia, PA 19111, USA*

[4]*Department of Chemistry University of Cambridge Lensfield Road, Cambridge CB2 1EW, and Centre for Protein Engineering, Medical Research Council Centre Hills Road, Cambridge CB2 2QH, UK*

**Corresponding author*

Heme-linked proteins, such as cytochromes, are popular subjects for protein folding studies. There is the underlying question of whether the heme affects the structure of the denatured state by cross-linking it and forming other interactions, which would perturb the folding pathway. We have studied wild-type and mutant cytochrome b_{562} from *Escherichia coli*, a 106 residue four-α-helical bundle. The holo protein apparently refolds with a half-life of 4 μs in its ferrous state. We have analysed the folding of the apo protein using continuous-flow fluorescence as well as stopped-flow fluorescence and CD. The apo protein folded much more slowly with a half-life of 270 μs that was unaffected by the presence of exogenous heme. We examined the nature of the denatured states of both holo and apo proteins by NMR methods over a range of concentrations of guanidine hydrochloride. The starting point for folding of the holo protein in concentrations of denaturant around the denaturation transition was a highly ordered native-like species with heme bound. Fully denatured holo protein at higher concentrations of denaturant consisted of denatured apo protein and free heme. Our results suggest that the very fast folding species of denatured holo protein is in a compact state, whereas the normal folding pathway from fully denatured holo protein consists of the slower folding of the apo protein followed by the binding of heme. These data should be considered in the analysis of folding of heme proteins.

Keywords: cytochrome b_{562}; heme; folding kinetics; continuous flow; NMR

Introduction

Heme-linked proteins, especially cytochrome *c*, have been favourite targets for protein folding studies because of their ready availability, large spectral changes associated with the heme, and the exploitability of its redox state. But, Wittung-Stafshede has reviewed the roles of cofactors in protein folding and has raised important questions about the influence of heme on protein folding studies.[1] The heme can play a crucial role in defining the folding properties of small cytochromes and globins, and attempts to rationalise these properties in terms of their sequence alone[2,3] should take this into account. The structure of the denatured state of a holo protein could be constrained by non-covalent and/or coordination links mediated by the heme. Also, how does one calculate the contact order of the heme-linked protein?[1] Some heme proteins fold independently of their cofactor to form an apo protein with an empty cofactor-binding site. Others require the cofactor to be present for productive and correct folding. Mitochondrial cytochrome *c* has no stable tertiary structure in the absence of heme,[4] which additionally must be covalently attached to the polypeptide for stability and function.[5] Myoglobin does fold in the absence of heme but some mutations that affect the stability of the apo protein do not affect the stability of the holo protein.[6] Cytochromes b_5 and b_{562} also fold in the absence of

Abbreviations used: DSC, differential scanning calorimetry; GdnHCl, guanidine hydrochloride; HSQC, heteronuclear single quantum coherence; ITC, isothermal titration calorimetry; NOE, nuclear Overhauser effect.

E-mail address of the corresponding author: pdb30@cam.ac.uk

0022-2836/$ - see front matter © 2005 Published by Elsevier Ltd.

heme[7,8] and are attractive subjects for study, since the structures of both the apo and holo proteins are available. But which species in the folding transition is relevant to our understanding of their folding mechanism; the denatured state in the presence or absence of heme? For both of these *b*-type cytochromes, the folded apo protein is thought to accumulate *in vivo* prior to heme insertion, although no direct evidence for this is available.

Cytochrome b_{562} from *Escherichia coli*, is a 106 residue, four-α-helical bundle protein containing a non-covalently bound *b*-type heme group.[9,10] The solution structure of apocytochrome b_{562}[11,12] contains the majority of the secondary structure of the holo form[9,10] but in a more open[12,13] and dynamic[13,14] state. Cytochrome b_{562} is translated with a leader peptide that directs the protein to the *Escherichia coli* periplasm before cleavage by a signal peptidase. It is not clear where in the cell the endogenous protein binds to heme, but when overexpressed with or without the leader peptide, the majority of the protein folds as the apo protein in the cells.[15] The rate constants for the refolding of ferrous holocytochrome b_{562} in the presence of varying concentrations of guanidine hydrochloride (GdnHCl) were extrapolated to give a value of $2\times 10^5\ s^{-1}$ at 20 °C in the absence of denaturant, the highest folding rate constant actually measured being $1500\ s^{-1}$.[16,17] The extrapolated rate constant approaches that of polymer intrachain diffusion ($5\times10^6\ s^{-1}$).[18–20] The rate of folding of holocytochrome b_{562} was measured by exploiting the difference in stability between its oxidised and reduced forms;[21] the transition from GdnHCl-denatured, oxidised b_{562} to native reduced b_{562} was triggered by photoinduced electron transfer[22] and the kinetics of the renaturation were measured by monitoring the absorption of the heme. Similar experiments have been used to study the folding of the related cytochrome *c* prime,[23] which shares the same fold of cytochrome b_{562} but has heme covalently attached to the polypeptide. The folding process of this protein was multiphasic over a large timescale.

These data raise important questions; what is the denatured state of the holo protein and what is the effect of oxidation state on it? Here, we describe the folding of the apo form of the protein and selected mutants, monitored by stopped-flow and continuous-flow fluorimetry, and by stopped-flow circular dichroism. We then examine, by NMR, the denatured state of the ferric holo protein, under the conditions used to study electron transfer-induced folding,[1,17] and find that two species existed under these conditions. One was a highly ordered native-like species with most residues in the same conformation as the native ferricytochrome and many heme-to-protein-residue nuclear Overhauser effects (NOEs) still observable. Further denaturation led to heme dissociation and a denatured state that looks the same as denatured apo protein. The fully denatured polypeptide did not appear to bind heme under these conditions and hence regeneration of the native holo protein required folding of the apo protein followed by heme binding. The difference in folding rate constants observed for apo and holo proteins are explained adequately, therefore, by a large difference in the starting points for the folding reaction.

Results and Discussion

Trp14, Trp61 and Trp65 as fluorescent probes

To improve the fluorescence of apocytochrome, folding-sensitive fluorescence probes were introduced into cytochrome b_{562}. We substituted tryptophan residues into positions in the structure where homology (with cytochromes *c*′)[24] and model building suggested that they would be tolerated (L14W, F65W and F61W in Figure 1). Positions 61 and 65 are located on helix 3 and are important for heme binding. Position 14 is located in a hydrophobic core that forms upon heme binding, but does not interact directly with the heme, and reports on the folding of helix 1. The F65W variant was also selected from a library of double mutants of cytochrome b_{562} that was screened for heme binding and hence folding efficacy.[25]

The stabilities of the Trp variants, measured by urea-denaturation followed by fluorescence or CD, heat-denaturation followed by CD and differential scanning calorimetry (DSC), spanned the value for the wild-type protein (Table 1). The equilibrium *m*-values for denaturation with urea were similar. The three variants had the same intrinsic CD spectrum as wild-type (data not shown) and a heme affinity close to that of wild-type (Table 1), demonstrating very similar overall protein structures. We conclude that the three mutants are sufficiently similar to the wild-type protein to

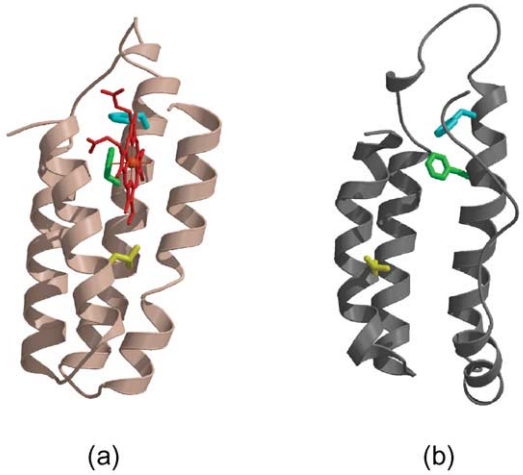

Figure 1. Ribbon representation of the NMR structure of (a) wild-type holocytochrome b_{562} (PDB code 1qpu)[10,11] and (b) *apo*-cytochrome b_{562} (PDB code 1apc).[12,13] The side-chains of Leu14, Phe 61 and Phe 65 are highlighted.

Table 1. Thermodynamic parameters for folding of wild-type apocytochrome b_{562} and its variants L14W, F61W, F65W at pH 7.0

Protein	[Urea] $_{50\%}$[a] (M)	$m_{D\text{-}N}$[a] (kcal mol^{-1} M^{-1})	$\Delta G^{H_2O}_{D-N}$[a] (kcal mol^{-1})	T_m[b] (K)	Heme dissociation[c] K_d (nM)
b_{562} WT	2.3[d]	1.4[d]	3.2±0.5	329	3.0
L14W	1.6±0.2	1.3±0.1	2.1±0.2	333.5	30
F61W	3.1±0.1	1.0±0.1	3.1±0.2	335	10
F65W	3.2±0.1	1.5±0.1	4.8±0.2	333	20

[a] $\Delta G = \Delta G^{H_2O}_{D-N} - m_{D-N}$[urea] at pH 7.0 K and 293 K.
[b] Determined by DSC at pH 7.0. Values are ±0.5 K.
[c] Determined by ITC at pH 8.0 at 298 K.
[d] From Hargrove *et al.*[7] and this work.

make them relevant reporters of the local and global folding events in apocytochrome b_{562}.

On excitation at 296 nm, the tryptophan variants gave emission spectra with maxima at 334 nm and at 329 nm for the native L14W and F65W, respectively. Spectra of the urea-denatured proteins are red shifted with maxima at 355 nm. At 320 nm, the fluorescence values of the urea-denatured states were only 30% and 17% of the fluorescence of the native state for L14W and F65W, respectively. The proteins are denatured reversibly by lowering the pH,[8] and so folding could be initiated by pH-jump. The proteins were unfolded at pH 1.5, as judged by the CD and fluorescence spectra, although the fluorescence spectrum of the acid-denatured protein was quenched significantly relative to the urea-denatured state.

Unfolding and refolding kinetics

Refolding of the acid-denatured apo proteins at pH 5.0 (pH of maximum stability of the wild-type protein) in the absence of urea at 293 K was extremely rapid and occurred within the dead-time of the stopped-flow fluorimeter. But the rate constants could be measured at 279 K. The amplitude of the folding process at 0 M urea was ~30% of that expected from the equilibrium change and consistent with the rate constant of the observed kinetic and the dead-time of about 1 ms. The refolding of wild-type b_{562} apo protein could be monitored by the weak fluorescent changes of the two tyrosine residues. At concentrations of denaturant greater than 1.0 M, the kinetics were monitored also by CD at 222 nm, a probe for α-helical secondary structure. The refolding rate constants of the Trp variants and wild-type in 1.2 M urea were within 15% of each other. At 1.2 M urea, the rate constant for the refolding of the wild-type protein was 150 s^{-1}, which is close to the value of 175 s^{-1} that was found for the change in CD signal. At pH 5.0, the pH jump-induced refolding of the variants monitored by tryptophan fluorescence, a probe for local environment, can be fit to a single-exponential function with an apparent rate constant of 1200(±200) s^{-1}(see Supplementary Material, Figure S1a). At 1.8 M urea, apparent refolding rate constants of 80 s^{-1} were measured (see Supplementary Material, Figure S1b and c). The refolding rate constants of F61W were very similar to those of F65W. Thermodynamic parameters obtained from kinetic and equilibrium experiments at pH 5.0 are summarised in Table 2.

The logarithm of the observed rate constant for refolding of L14W and F65W varied linearly with concentration of urea from 0.6 M to 1.8 M or 3 M, respectively (Figure 2). The values deviated significantly below 0.6 M urea from those predicted by the kinetics of a two-state equation. This was evident for the existence of a folding intermediate on the refolding pathway.[26,27] At higher concentrations of urea (0.8–7 M), the unfolding and refolding rate constants fitted a two-state model (Figure 2). The fact that the L14W mutant folds at the same rate suggests that the probe on helix 1 is sensitive to the same processes as the probes on helix 3.

We used fast continuous-flow fluorescence methods to measure a refolding rate constant of of 2600 s^{-1} for F65W at 294 K in the absence of denaturant (Figure 3).[28,29] This rate constant is about twice as high as that measured at 279 K, which is reasonable for this increase in temperature. While there is no evidence for another kinetic phase in these data, the phase that occurs with a rate constant of 2600 s^{-1} accounts for only about half of the total equilibrium change in fluorescence. The baseline fluorescence measured at pH 1.5 (Figure 3), where the fluorescence of tryptophan is quenched strongly by protons,[30] does not reflect the true fluorescence of the denatured protein at pH 5, which is the true starting point for folding. The initial fluorescence signal under these conditions had to be estimated by extrapolation of the dependence on urea of the fluorescence spectrum of the denatured state of F65W to 0 M urea. From this, we conclude that the burst amplitude observed in this experiment is consistent with the effect of pH upon the fluorescence of the denatured protein and there are no other fast kinetic phases to account for. The rate constants for folding measured at 279 K and 294 K are consistent with data extracted from relaxation measurements using temperature-jump experiments in the thermal unfolding transition between 315 K and 335 K (data not shown).

Table 2. Thermodynamic parameters from equilibrium and kinetic experiments on wild-type apo-cytochrome b_{562} and its variants L14W, F61W, F65W at pH 5.0

	$[Urea]_{50\%}$ (M)		m_{D-N} (kcal mol^{-1} M^{-1})		m_k[a] (kcal mol^{-1} M^{-1}) (279 K)	ΔG[b] (kcal mol^{-1})		$\Delta G^{H_2O}_{D-N}$[c] (kcal mol^{-1}) (279 K)	T_m[d] (K)	ΔH_{cal}[d] (kcal mol^{-1})	ΔH_{vH}[d] (kcal mol^{-1})
	279 K	293 K	279 K	293 K		279 K	293 K				
WT	3.0±0.1	–	1.6±0.1	–	–	4.8±0.2	–	–	328	46±4	56±4
L14W	2.6±0.1	–	2.0±0.3	–	3.9±0.5	5.2±0.5	–	4.7±0.4	327	44±4	52±3
F61W	–	3.2±0.1	–	1.2±0.2	–	–	3.9±0.4	–	335	66±4	62±4
F65W	3.4±0.1	3.2±0.1	1.7±0.2	1.2±0.2	3.3±0.2	5.8±0.4	3.7±0.4	5.2±0.5	335	64±6	63±5

[a] $m_k = m_{kf} + m_{ku}$.
[b] $\Delta G = \Delta G^{H_2O}_{D-N} - m_{D-N}[urea]$.
[c] $\Delta G^{H_2O}_{D-N} = RT \times \ln\left(\frac{k_f^{H_2O}}{k_u^{H_2O}}\right)$.
[d] Determined by DSC at pH 5.0. Values of T_m are ±0.5 K.

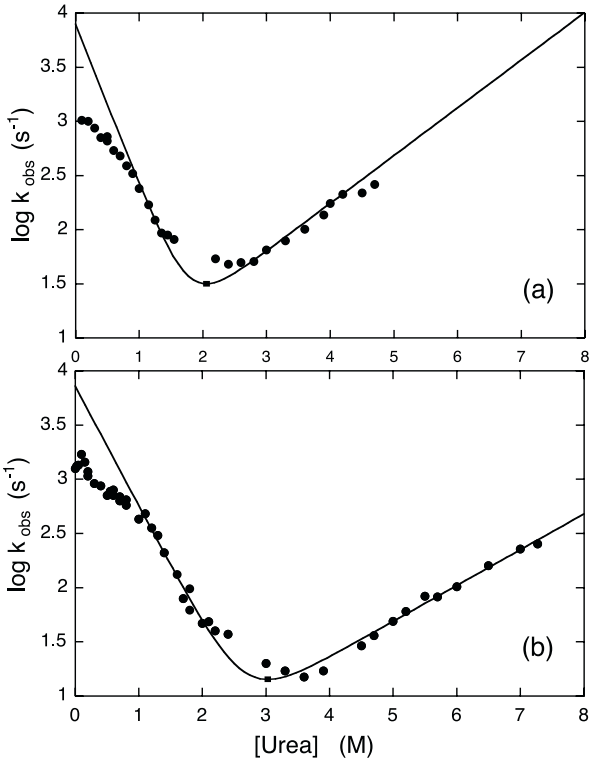

Figure 2. Urea concentration dependence of the logarithm of the apparent rate constant (k_{obs}) of refolding and unfolding for (a) L14W and (b) F65W. The continuous lines represent the fit of the data around the mid-point to a two-state model.

Equilibrium denaturation of holocytochrome b_{562} monitored by different probes

The presence of the heme chromophore makes the monitoring of denaturation of cytochromes apparently facile. But what do changes in the heme absorbance report? For cytochrome b_{562}, the equilibrium denaturation of both ferric and ferrous holo protein appears to be a two-state process.[1,31] We have measured the denaturation of the ferric holo protein by steady-state CD and this also reports two-state folding (Figure 4). We have examined the effect of denaturant on the NMR spectra of the ferric holo protein. The 1D ^{1}H spectra, encompassing paramagnetic and diamagnetic resonances of heme and protein protons, and ^{15}N-^{1}H HSQC spectra were collected at 16 different concentrations of GdnHCl up to 4 M at the same pH (7.0) as that used in the holo protein folding experiments. The averaged volumes of the amide protons assigned on the ^{15}N-^{1}H HSQC spectra are plotted also as a function of denaturant concentration in Figure 4. The intensity of the heme methyl proton resonances (plotted using the most shifted signals on the 1D spectra) showed behaviour (not shown) essentially identical with that of the protein amide protons. These data cannot be fit to a simple two-state equilibrium and report another process,

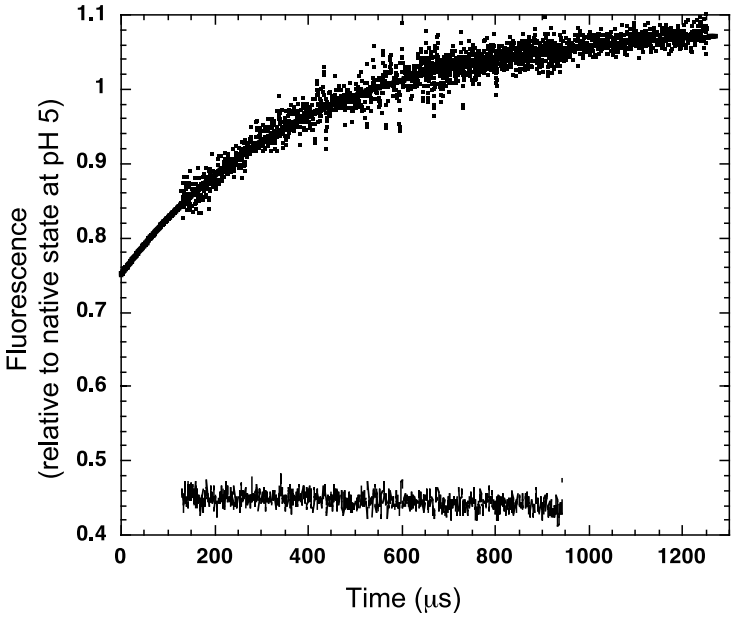

Figure 3. Kinetic traces of the folding at 294 K at pH 5.0 of F65W apocytochrome b_{562} obtained from continuous-flow fluorescence experiments. Data from two separate experiments (dots) collected from two timescales (see Materials and Methods) were merged and fit to a single, first-order exponential function (thick continuous line, rate constant 2600 s^{-1}) by least-squares analysis. The baseline fluorescence of denatured protein (from 130–940 μs) is shown (thin line).

occurring between 0 M and 2 M denaturant. From the denaturant concentration-dependence of the intensity of selected individual amide proton resonances in the ^{15}N-^{1}H heteronuclear single quantum coherence (HSQC) (Figure S2), it is clear that changes in the protein are not very cooperative. A qualitatively similar plot results if amide chemical shifts are plotted against denaturant concentration (data not shown). These changes in the ^{15}N-^{1}H HSQC are mirrored also by small but significant changes in chemical shifts of the paramagnetically shifted resonances of the heme substituent protons, but all of these changes could be accounted for simply by effects of increased ionic strength of the solvent on the probe sensitivity.[32]

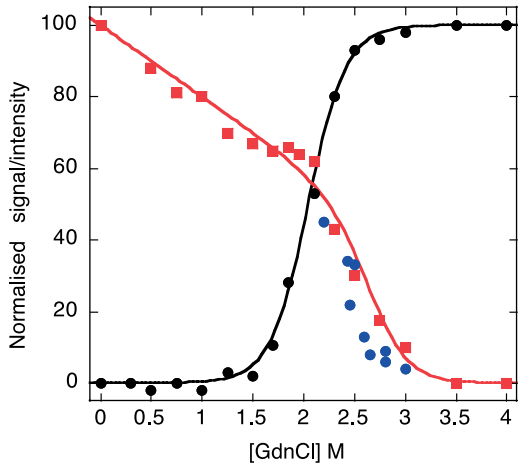

Figure 4. Equilibrium denaturation of holocytochrome b_{562} with GdnHCl measured by CD (black circles), and HSQC peak volumes (red squares). Superimposed on this are the amplitudes of kinetic traces of electron transfer triggered folding of holo protein (from Wittung-Stafshede *et al.*,[17] blue circles).

Characterisation by NMR of ferric holocytochrome b_{562} at 2 M GdnHCl

^{15}N-^{1}H HSQC spectra at 0 M, 2 M and 3 M GdnHCl are shown in Figure 5. While the spectra at 0 M and 3 M denaturant (Figure 5(a) and (c)) are consistent with single species in each, corresponding to the native holo protein and denatured apo protein, respectively, the spectrum at 2 M denaturant (Figure 5(b)) is indicative of a mixture of two species that are in very slow equilibrium. The signals from the species labelled in red correspond exactly to those of the apocytochrome measured under the same conditions and were entirely consistent with completely denatured protein due to the similarity to random-coil shift values (Figure 6(a)). The dispersion of the resonances associated with the other species (labelled in blue in Figure 5(b)) is consistent with a compact folded state, but the chemical shifts of this species are different from those of the native holo or apo proteins or of the denatured apo protein. We have assigned almost all of the amide and H^{α} protons in this new species under these conditions. The variation in the H^{α} chemical shifts from random-coil values for the ferric holo protein at 0 M and 2 M GdnHCl, shown in Figure 6(b) and (c), are similar and suggest that this form in 2 M GdnHCl still retains most of the secondary structure elements of the native state. Comparison between the chemical shifts of these species, labelled green and blue in Figure 5, shows little significant variation overall (Figure 6(d)). A few NH resonances disappear from the HSQC spectra at 2 M GdnHCl; among them, it is worth mentioning those of His102 and Met7, which are barely detected even in the absence of GdnHCl.

So what is different about the protein at 2 M GdnHCl compared with the native state? While all H^{α}, HN, and ^{15}N chemical shifts (Figure 6; and see Supplementary Material, Figure S3) were not

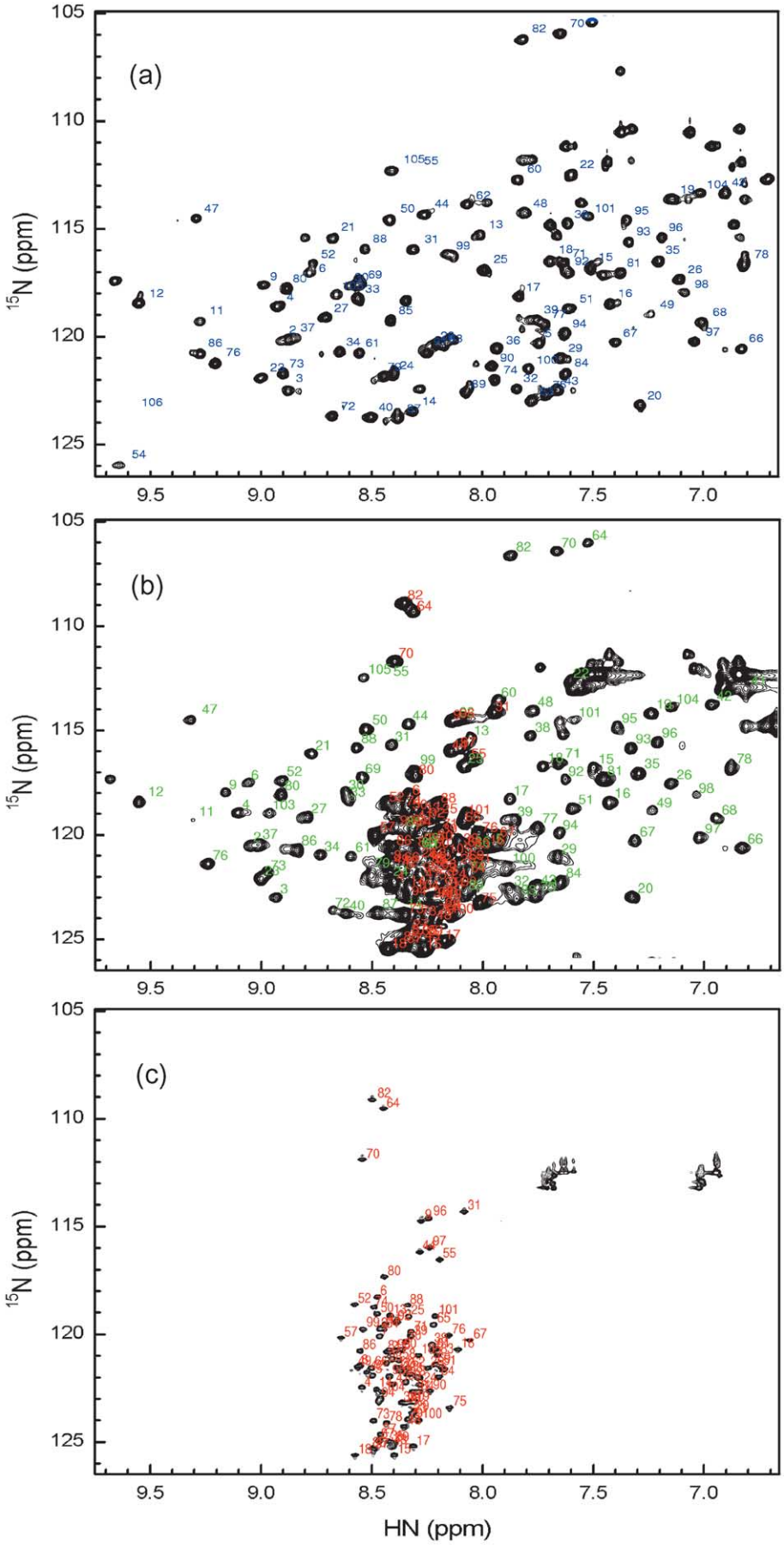

Figure 5 (*legend opposite*)

globally altered between the two conditions, the H^{α} showed larger changes at the termini of the protein and in helix 2. The pattern of $d\alpha N(i,i+3)$ NOEs observed in the 3D NOESY experiment (Figure 6(b) and (c)) reveals that the majority of the α-helical content of the native protein is still present in 2 M GdnHCl. There were, however, some differences in the medium-range NOEs observed in certain regions of sequence when compared with those observed in the native state.[9] Notably, residues 3–15 and 88–100 (in the sequences around the ligand residues, 7 and 102 at either terminus of the protein) no longer gave $d\alpha N(i,i+3)$ NOEs indicative of α-helical conformation. Additionally, there is a gap (residues 33–38) in the helical pattern corresponding to helix 2 (22–42) of the native protein. Helix 3 (residues 62–82) of the native protein appeared completely intact in this species. The structure of the native ferricytochrome solved at pH 7 (B.L., Bertini I. & C.-B.S., unpublished results) is identical, within the experimental error, with that at pH 4.8 as described.[9]

The decrease in intensity of some NH signals observed from 0–2 M GdnHCl are consistent with a reduction of the helical content of ~30% in the native-like species. On the contrary, the CD titration indicates a 50% reduction of α-helices that might correspond to a combination of the local unfolding generating the native-like species characterised here, and the complete unfolding of the protein. CD (and for that matter absorbance) cannot resolve this three-state equilibrium.

This species in 2 M denaturant still had heme bound in an environment similar to that of the native state, as indicated clearly by the characteristic hyperfine-shifted signals of the ^{1}H NMR spectra (Supplementary Material, Figure S4). This is supported by the fact that many of the NOEs observed between the porphyrin protons and protein residue protons can still be observed in 2 M GdnHCl (Figure 7). These data suggest that the electronic structure of the iron porphyrin is altered only subtly when compared with the native state in the absence of GdnHCl.

We have performed a ^{15}N backbone dynamics analysis of the ferric holo protein at 0 M and 2 M GdnHCl. Overall, the values of the relaxation parameters R_1 and R_2 between the two protein states are rather similar, confirming that no global change in conformation had occurred (Supplementary Material, Figure S5). On the other hand, the heteronuclear NOE values are quite different (Figure 8). The native state is notable for being a rather rigid molecule,[14] even at the termini, which are restricted from movement not by specific secondary structure, but by the coordination of residues 7 and 102 to the heme iron. Figure 8(b) shows that in 2 M GdnHCl, the terminal stretches of sequence 1–10 and 97–106 are clearly more mobile.

The denaturing effect of GdnHCl on the structure and dynamic properties of another *b*-type cytochrome, as analysed through NMR applied to the oxidized state of the A-form of rat microsomal cytochrome b_5, has been reported.[33,34] The structural characterization of cytochrome b_5 in the presence of 2 M GdnHCl showed that the overall fold of the protein is still maintained and few structural changes are detected, as it is the case here with cytochrome b_{562}. Moreover, mobility studies on oxidized cytochrome b_5 in the presence of 2 M GdnHCl[34] show an increase in mobility upon addition of denaturant occurring largely around the heme pocket, as it is observed for cytochrome b_{562}.

What is the starting point for folding of holo protein?

The rate constant for the refolding of ferrous holocytochrome b_{562} is about 800 s^{-1} in 2.5 M GdnHCl and 293 K.[16] The rate constants measured between 2.2 M and 3.0 M GdnHCl extrapolate to 2×10^{5} s^{-1} in 0 M denaturant,[17] tending to the predicted limit for the formation of helices,[18–20] and nearly 100 times faster than the folding of F65W apo protein at 294 K. This extrapolated rate constant for the ferrous holo protein is extremely high. The refolding rate constant for the engrailed homeodomain three-helix protein, the highest yet measured directly in the absence of denaturant, is some four times lower under optimal conditions.[35] However, plotting the amplitude of the single kinetic phase observed in these experiments[17] as a function of the concentration of denaturant (Figure 4) revealed that this amplitude corresponds to the population of native-like species as deduced by the intensity of the corresponding signals in the ^{15}N-^{1}H HSQC spectra. We therefore equate the starting point for the electron transfer-initiated folding studies with the native-like, ferric holo protein species we have characterised here by NMR. Clearly, therefore, the changes in heme absorbance monitored previously[16,17] do not report any global change in the protein fold. Rather, they report coordination changes to the heme iron. From the change in absorption spectrum with increasing concentrations of denaturant (data not shown)[16,17] we would suggest that the ligands are not coordinated to the iron, although it is most likely that they are coming on and off the metal. This would help to explain the disappearance of NMR signals, particularly of the amide protons of the ligand residues upon addition of GdnHCl. A similar consequence is observed when the coordination to heme iron is

Figure 5. ^{1}H-^{15}N HSQC spectrum of cytochrome b_{562} in (a) 0 M, (b) 2 M and (c) 3 M GdnHCl, at pH 7 and 20 °C. Signals corresponding to native, folded holo protein are labelled with residue number in blue. Signals associated with the compact, native-like, folded species are labelled with residue number in green. Signals corresponding to denatured apocytochrome are labelled with residue number in red.

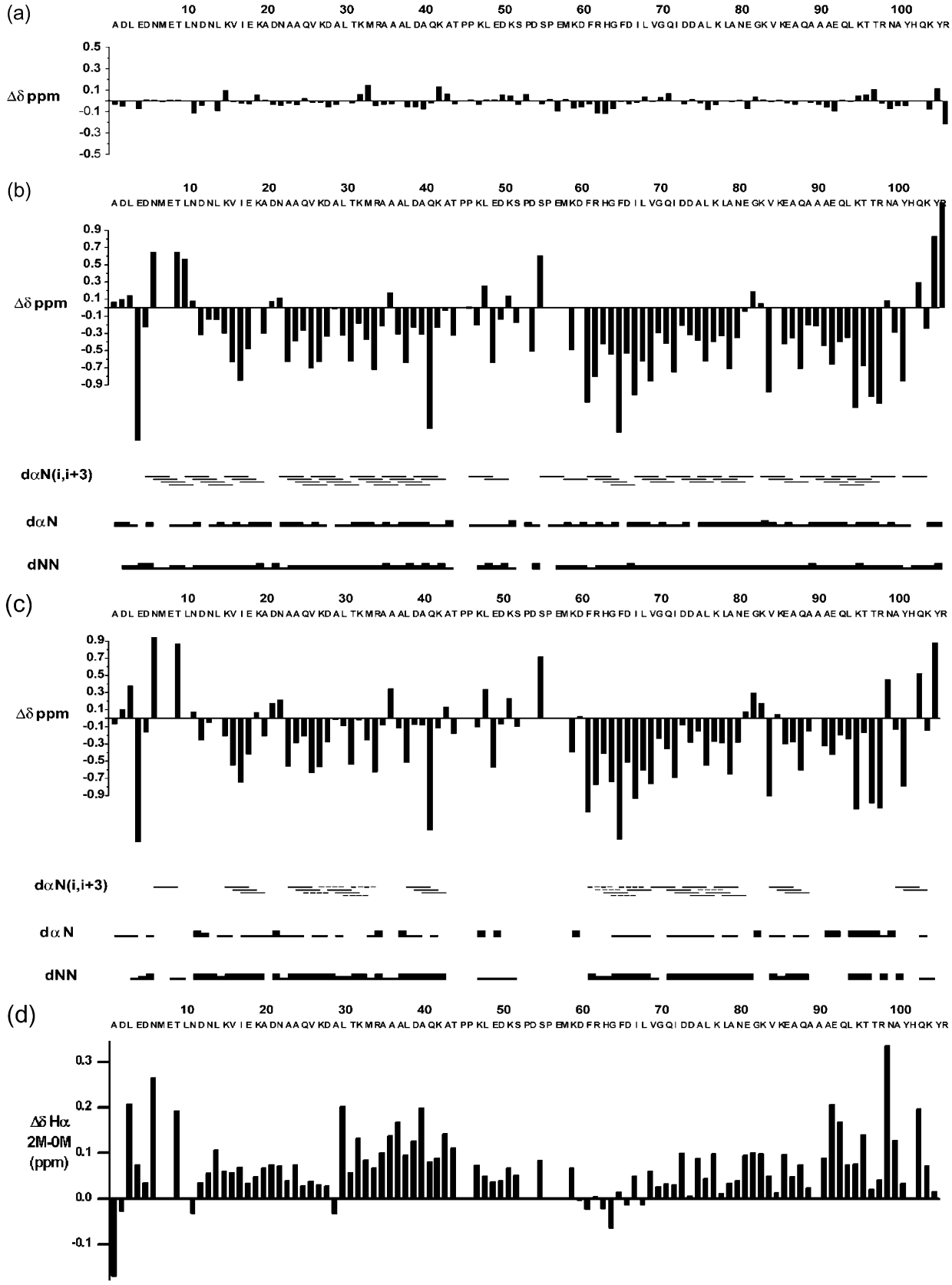

Figure 6. H^{α} chemical shift deviation from random-coil values (conformational shifts; $\Delta\delta = \delta_{experim} - \delta_{random\ coil}$) as a function of the sequence for cytochrome b_{562} in various conditions: (a) apo protein in 2 M GdnHCl, (b) holo protein in the absence of GdnHCl and (c) holo protein in 2 M GdnHCl. (d) H^{α} chemical shifts differences between holocytochrome b_{562} in 2 M GdnHCl and in the absence of GdnHCl as a function of the sequence. For the holo protein in (b) the absence of GdnHCl and (c) 2 M GdnHCl, a summary of sequential ($d\alpha$N and dNN) and medium-range ($d\alpha$N(i,i+3)) NOEs involving H^{α} and NH protons is presented.

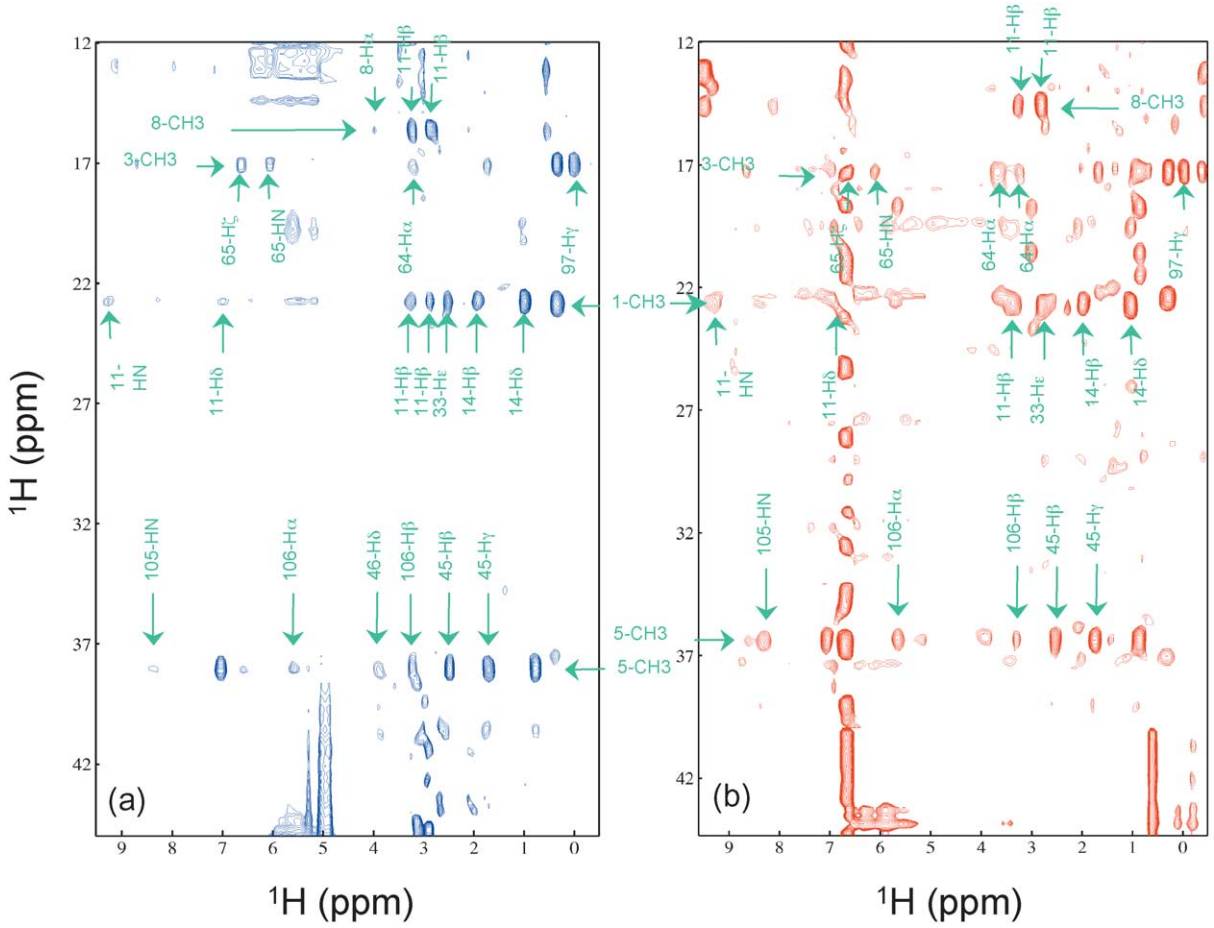

Figure 7. ^{1}H NOESY spectrum of holocytochrome b_{562} in (a) the absence of GdnHCl and (b) 2 M GdnHCl, showing interactions between residues of the polypeptide chain (chemical shifts located between 0 ppm and 10 ppm) and the methyl groups from the porphyrin ring (chemical shifts located between 12 ppm and 42 ppm).

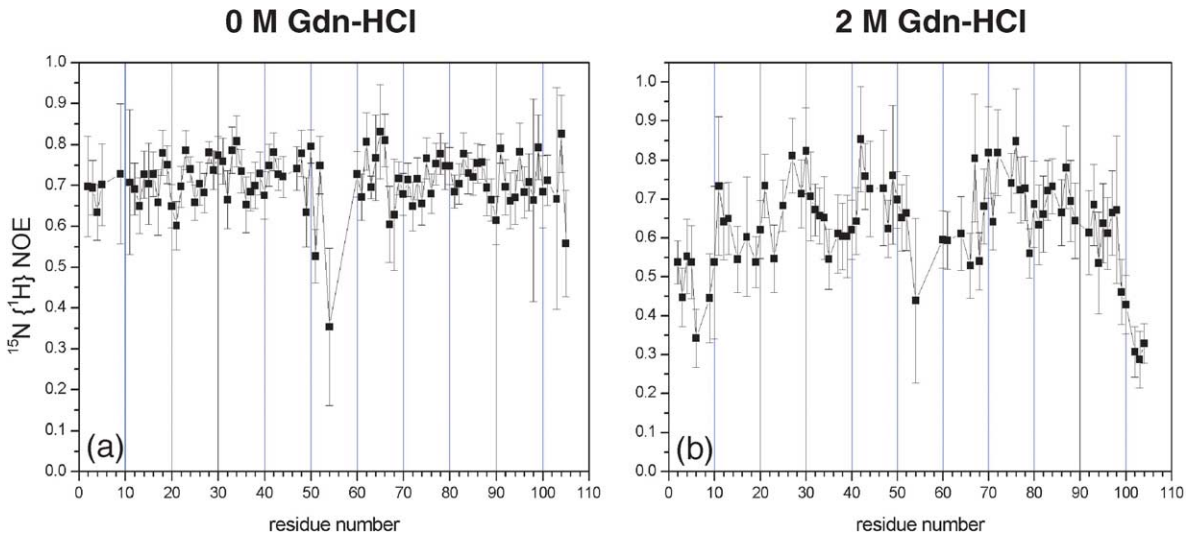

Figure 8. Heteronuclear ^{15}N-{^{1}H}NOEs of backbone amide groups from holocytochrome b_{562} in (a) the absence of GdnHCl and (b) 2 M GdnHCl, recorded on an Advance Bruker spectrometer working at a ^{15}N resonance of 60 MHz.

weakened by mutagenesis of the ligands.[36,37] It has been suggested that changes in co-ordination to the heme iron are not related to any folding events in cytochrome *c*.[38] In this current example of cytochrome b_{562}, the changes in the protein fold and mobility that result in this weakening or loss of heme iron ligands appear to be limited mainly to the terminal stretches of sequence around these ligands, residues 1–15 and 88–106 (coloured yellow in state A in Figure 9). The folding of the ferrous holo protein[16,17] was initiated by reduction of the ferric protein in this compact state. Therefore, the rates measured probably represent the completion of helices 1 and 4 in these terminal regions and the anchoring of the ligands to the heme iron.

Folding of the apo protein?

The folding of the apo protein does begin from an extensively denatured state and, presumably, consequently is nearly two orders of magnitude slower than the process observed under the same conditions for the ferrous holo protein. It is notable that the relative compactness of the 2 M GdnHCl state of the ferrous holo protein could have been predicted from the comparison of the thermodynamic data for the apo and holo proteins. Compactness in a denatured state can sometimes be detected from the equilibrium *m*-value for denaturation, which is derived from plots of free energy of denaturation against denaturant concentration that often follow the equation:

$$\Delta G_{D-N} = \Delta G^{H_2O}_{D-N} - m[\text{Denaturant}]$$

where $\Delta G^{H_2O}_{D-N}$ is the free energy of denaturation in water. The *m*-value is a measure of the change in surface area upon denaturation. The *m*-values in GdnHCl for the denaturation of apo, ferric and ferrous holocytochrome b_{562} are 3.4 kcal mol^{-1} M^{-1}, 3.3 kcal mol^{-1} M^{-1} and 1.8 kcal mol^{-1} M^{-1}, respectively (1 cal = 4.184 J) (our unpublished results, and see Wittung-Stafshede *et al.*[17]). These data suggest that the ferrous denatured state is significantly more structured and compact than the ferric state. The *m*-value for the ferric holo protein, obtained from titrations monitored by CD or absorbance, has no contribution from the native-like species we have characterised, and therefore reflects the fact that ultimately the native, ferric holo protein is denatured to the apo protein plus free heme. We have previously studied variants of cytochrome b_{562} in which the heme is covalently attached to helix 4 through cysteine residues at positions 98 and 101.[15,31] The electronic spectra of the GdnHCl-denatured state of the ferric form of these variants show that the heme is still in a somewhat structured environment in these proteins. The *m*-values for the unfolding of the ferric state of these proteins in GdnHCl are 1.8–2.0 kcal mol^{-1} M^{-1} (our unpublished results),[31] values similar to that of the ferrous, wild-type cytochrome b_{562} holo protein. Finally, as a result of calorimetric studies, it has been suggested that heme is still associated with the thermally denatured state of ferric cytochrome b_{562} (K_d 6 μM).[39,40] All the thermodynamic evidence suggests that the apparently denatured state of the reduced cytochrome is clearly more collapsed, as we have revealed by our NMR analysis.

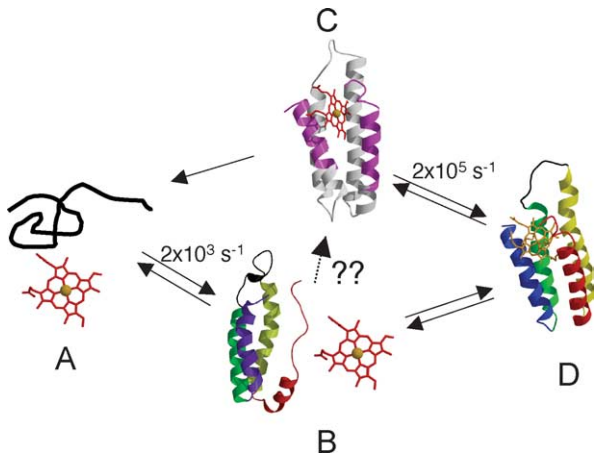

Figure 9. Cartoon of a folding scheme for cytochrome b_{562}. State A refers to unfolded protein and "free" heme in 3 M denaturant. State B refers to folded apo protein and "free" heme in the absence of denaturant. State C refers to ferric holo protein in the presence of 2 M GdnHCl and state D refers to the native holo protein in the absence of denaturant.

Implications for studies on protein folding

The observations that heme causes compaction of the denatured state of cytochrome b_{562} and that apocytochrome b_{562} folds much more slowly than previously reported, implies that heme-linked proteins have idiosyncratic folding behaviour. The folding of the apo protein is the most relevant for fundamental folding studies, even if there are significant conformational and dynamic differences between apo and holo proteins. Since heme is a crucial determinant of both the equilibrium and kinetic folding properties of cytochrome b_{562}, the inclusion of this protein and, by inference other heme proteins, in correlation analyses relating sequence or topology to folding kinetics should be considered only with qualifications. Thus, if the measured rate constants for folding both the holo- and apocytochromes b_{562} are plotted in a graph of log k_f *versus* contact order,[2] the apocytochrome folding rate constant correlates with a contact order of 13% rather than the 7% for the holo protein. The heme cofactor needs to be included as a contributor to an increased apparent contact order. However, this point is moot: a plot against contact order of the logarithm of rate constants for folding of a wide range of two-state proteins shows an enormous scatter, because both contact order and the stability of the transition state contribute to the rate constant for folding.[41,42]

Because the only other species observed in our NMR analysis of the denaturation of cytochrome

b_{562} is the denatured apo protein, and we can find no effect of exogenous heme on the rate of folding of the apo protein, we suggest that the folding of the fully denatured holocytochrome proceeds only by the initial folding of the apo protein followed by the binding of heme (Figure 9). The equilibrium folding of the apo protein monitors states A and B, while that of the holo protein monitors A and C, not A and D. Kinetically, the folding pathway from A to D almost certainly proceeds *via* state B, with the overall rate-determining step being heme binding, B to D. Circumstances in which states B and C are the stable forms of this system, in the absence of denaturant, probably arise when there is no ligand available for the heme. This can be addressed by removal of the ligands by mutagenesis. The effects of heme on cytochrome b_{562} are likely to be replicated with other heme-linked proteins, in particular where the heme is bound covalently, such as with cytochrome *c*. In general, there should be extreme caution in extrapolating early events in the folding of heme-linked proteins to the folding of other proteins.

Materials and Methods

Cloning and mutagenesis

The mutations L14W, F61W, F65W were introduced into the cytochrome b_{562} gene using the Stratagene Quickchange method. The plasmids were isolated and the expected sequence was confirmed by standard dideoxynucleotide sequencing. Cytochrome b_{562} was expressed from plasmid pPB10 in *E. coli* (strain NM554 or TG2). Apocytochrome b_{562} was isolated and purified as described.[15,36] Molar extinction coefficients at 282 nm of 8380 M^{-1} cm^{-1}, 8450 M^{-1} cm^{-1} and 8960 M^{-1} cm^{-1} were determined for L14W, F61W and F65W, respectively.[43]

Stopped-flow, pH-jump refolding and stopped-flow urea-unfolding experiments

Refolding experiments were carried out with solutions of the tryptophan variants at between 2 μM and 30 μM denatured in 30 mM HCl (pH 1.5). Rapid 1:1 (v/v) mixing of this solution with refolding buffer (200 mM potassium acetate (pH 5.8), 200 mM KCl) yield a final protein concentration of ~4 μM in 0.1 M potassium acetate buffer at pH 5.0. For the unfolding experiments, protein solutions of ~40 μM were prepared in potassium acetate buffer and mixed rapidly in a 1:10 (v/v) ratio with the same buffer at different concentrations of urea. All experiments were performed using a modified Applied Photophysics SX.18MV or an Applied Photophysics PiStar-180 stopped-flow spectropolarimeter-fluorimeter apparatus. The reservoir, syringes and the cuvette were maintained at a constant temperature of 279(±1) K. The fluorescent changes upon refolding or unfolding were monitored using an excitation wavelength of 296 nm and the emission was collected at wavelengths greater than 320 nm using a cut-off window filter. The CD changes were monitored at 222 nm.

Continuous-flow, pH-jump refolding experiments

Refolding experiments were performed using the continuous-flow instrument described elsewhere.[44] Denatured F65W at 110 μM in 100.4 mM HCl was mixed in a 1:10 (v/v) ratio with 30 mM potassium acetate (pH 5.0), 80 mM KCl, giving a final refolding concentration of 10 μM protein. The ionic strength of the protein solution (0.1 M) is therefore constant during mixing. The refolded protein was collected and passed through the instrument under identical conditions to obtain the fluorescence level of the native state. All data were normalised to this value. The data were collected over two timescales (130–940 μs and 650–1250 μs) by imaging separately two regions of the cuvette in separate experiments. The normalised data were merged and fit to a single-exponential function.

Calorimetry

Differential scanning calorimetry (DSC) measurements were performed using a MicroCal VP-DSC, the temperature was ramped from 293–363 K at a scan rate of 60 K $hour^{-1}$. Apocytochrome proteins were prepared to ≈1 mg ml^{-1} in the reference solution (0.1 M potassium acetate (pH 5), 0.1 M KCl). From the DSC thermograms, the midpoint temperature of the thermal unfolding transition, the calorimetric (ΔH_{cal}) and van't Hoff enthalpy (ΔH_{vH}) of denaturation were obtained using the Origin software version 4.1 from MicroCal Software Inc, USA. Isothermal titration calorimeter (ITC) measurements were performed using a MicroCal VP-ITC: 250 μM heme in 20 mM bicine, 1 mM EDTA solution was titrated in the 15 μM protein solution in the same buffer at a constant temperature of 293 K. Before the experiments, the samples were degassed under vacuum with gentle stirring for five minutes. The protein concentrations were determined by measuring absorbance at 282 nm using a Cary 500 UV-Vis-NIR or a Hewlett Packard 8453 spectrophotometer.

Equilibrium unfolding

For equilibrium unfolding experiments, native apo or holo protein in either 0.1 M potassium acetate buffer (pH 5.0) or 0.02 M sodium phosphate (pH 7) with the ionic strength adjusted to 0.1 M with NaCl, was diluted 1:10 (v/v) with the same buffer containing different concentrations of urea and incubated at 279 K or 293 K for at least two hours. The denaturation curves were monitored by fluorescence on an Aminco Bowman series 2 luminescence spectrometer (excitation wavelength: 296 nm) or by CD using a Jasco J-720 spectropolarimeter. The acid-denaturation curves, at a constant ionic strength of 0.1 M, were also monitored by fluorescence on a Molecular Dynamics Gemini Plus 96-well plate fluorimeter, using an in-house-modified water-thermostatically controlled plate-holder and a quartz 96-well plate (Hellma).

NMR methods

All experiments were performed in 20 mM potassium phosphate buffer containing 80 mM KCl at pH 7 at 20 °C. A minute amount of sodium 3-trimethylsilyl(2,2′,3,3′-$^2H_4$)-propionate (TSP) was added to the sample as an internal chemical shift reference.

Sequential assignment of apocytochrome b_{562} in 2 M GdnHCl and holocytochrome b_{562} in 0 M and 2 M GdnHCl

The NMR spectra were acquired on Avance 800, 700 and 600 Bruker spectrometers operating at a proton nominal frequency of 800.13 MHz, 700.13 MHz and 600.13 MHz, respectively. All the triple resonance (TXI 5 mm) probes used were equipped with pulsed field gradients along the *z*-axis. The 3D ^{15}N-HSQC-TOCSY, ^{15}N-HSQC-NOESY and HNHA spectra[45,46] were used for the sequential assignment of apocytochrome b_{562} in 2 M GdnHCl and holocytochrome b_{562} in 0 M and 2 M GdnHCl. All spectra were acquired in TPPI mode. ^{15}N-HSQC-TOCSY and ^{15}N-HSQC-NOESY spectra were recorded with mixing times of 80 ms and 100 ms, respectively, with data sets comprising 256(^{1}H)×64(^{15}N)×2048(^{1}H) data points. The HNHA experiment[46] was recorded with 128(^{1}H)×60(^{15}N)×2048(^{1}H) data points.

All NMR data were processed using standard Bruker software and analyzed using NMRView software.[47] Forward linear prediction was used in the ^{15}N dimension and the 3D data sets were zero-filled. For apocytochrome b_{562} in 2 M GdnHCl, 91 amide ^{15}N and attached protons out of 101, after discounting the N terminus and the four proline residues, as well as 101 H^{α} resonances were assigned. For holocytochrome b_{562} in 0 M GdnHCl at pH 7, 96 amide ^{15}N and attached protons out of 101, as well as 98 H^{α} resonances were assigned. For holocytochrome b_{562} in 2 M GdnHCl at pH 7, 89 amide ^{15}N and 93 attached protons out of 101, as well as 95 H^{α} resonances were assigned.

Equilibrium unfolding transition

Denaturation as followed by NMR was performed by adding small amounts of 8 M GdnHCl stock solution into an NMR tube containing 2 mM oxidized holo protein. Protein concentration was maintained at its initial value by adding small amounts of a protein stock solution at the same time that GdnHCl was added. Samples were left to equilibrate for 20 minutes before recording spectra. At each concentration of GdnHCl, a ^{1}H-^{15}N HSQC spectrum and a 1D spectrum with a spectral width of 80 ppm and with a recycle time of 300 ms were recorded. In addition, to detect connectivities between hyperfine shifted signals, a 2D NOESY experiment[48,49] with a spectral width of 80 ppm in both frequency dimensions, with 50 ms of mixing time, and with a recycle time of 200 ms was acquired on the 600 MHz spectrometer for the ferricytochrome b_{562} in 0 M and 2 M GdnHCl. The apo protein was studied in the same buffer containing 2 M GdnHCl at a final protein concentration of 2 mM.

^{15}N relaxation experiment

^{15}N R_1, R_2, and steady-state heteronuclear NOEs were measured with pulse sequences as described.[50] The ^{15}N transverse relaxation rates, *R*2, were measured by using the Carr-Purcell-Meiboom-Gill (CPMG) sequence.[51] Longitudinal and transverse relaxation rates were obtained using delays in the pulse sequence ranging from 5–1500 ms and from 16.96–288.32 ms, respectively. A refocusing delay of 450 μs was used in the transverse relaxation measurements. A recycle delay of 3 s was used for R_1 and R_2. For heteronuclear ^{1}H-^{15}N NOE measurements, 2D spectra were acquired using the water flip-back method to suppress the water resonance and avoid saturation of the amide resonances. The steady-state heteronuclear ^{1}H-^{15}N NOE was obtained by recording spectra with and without proton saturation. In the case of reference spectra without proton saturation, a relaxation delay of six seconds was employed, whereas a delay of three seconds before the three seconds of proton saturation was employed for spectra with proton saturation.

In all, 1024×256 data points were collected for each map, using eight scans for each experiment. Quadrature detection in *F*1 was obtained by using the TPPI method. Integration of cross-peaks for all spectra was performed by using the standard routine of the XWINNMR program.

Relaxation rates R_1 and R_2 were determined by fitting the cross-peak volumes, measured as a function of the delay within the pulse sequence, to a single-exponential decay. Standard deviations of the data from the fitted line were used as errors on the rates. Heteronuclear ^{1}H-^{15}N NOE values were calculated as the ratio of peak volumes in spectra recorded with and without ^{1}H saturation. The heteronuclear ^{1}H-^{15}N NOE values and their errors were estimated by calculating the mean ratio and the standard error from the available data sets.

Acknowledgements

This work was supported by the BBSRC under the SBDA initiative, the EU TMR Life Sciences programme (contract ERBFMRX-CT-98-0230), the MRC and the NIH (grant GM056250 to H.R.). P.D.B. thanks the BBSRC for an Advanced Research Fellowship. We thank Dr Margarida Gairi for the acquisition of spectra on the 800 MHz NMR spectrometer at the Parc Cientific de Barcelona.

Supplementary Data

Supplementary data associated with this article can be found, in the online version, at doi: 10.1016/j.jmb.2004.11.044

References

1. Wittung-Stafshede, P. (2002). Role of cofactors in protein folding. *Accts Chem. Res.* **35**, 201–208.
2. Baker, D. (2000). A surprising simplicity to protein folding. *Nature*, **405**, 39–42.
3. Plaxco, K. W., Simons, K. T., Ruczinski, I. & Baker, D. (2000). Topology, stability, sequence, and length: defining the determinants of two-state protein folding kinetics. *Biochemistry*, **39**, 11177–11183.
4. Stellwagen, E., Rysavy, R. & Babul, G. (1972). The conformation of horse heart apocytochrome *c*. *J. Biol. Chem.* **247**, 8074–8077.
5. Barker, P. D. & Ferguson, S. J. (1999). Still a puzzle: why is haem covalently attached in *c*-type cytochromes? *Structure*, **7**, R281–R290.
6. Hargrove, M. S., Krzywda, S., Wilkinson, A. J., Dou, Y., Ikeda-Saito, M. & Olson, J. S. (1994). Stability of myoglobin: a model for the folding of heme proteins. *Biochemistry*, **33**, 11767–11775.

7. Feng, Y. Q. & Sligar, S. G. (1991). Effect of heme binding on the structure and stability of *Escherichia coli* apocytochrome b_{562}. *Biochemistry*, **30**, 10150–10155.
8. Manyusa, S. & Whitford, D. (1999). Defining folding and unfolding reactions of apocytochrome *b*(5) using equilibrium and kinetic fluorescence measurements. *Biochemistry*, **38**, 9533–9540.
9. Arnesano, F., Banci, L., Bertini, I., Faronoe-Mennella, J., Rosato, A., Barker, P. D. & Fersht, A. R. (1999). The solution structure of oxidized *Escherichia coli* cytochrome b_{562}. *Biochemistry*, **38**, 8657–8670.
10. Hamada, K., Bethge, P. H. & Mathews, F. S. (1995). Refined structure of cytochrome b_{562} from *Escherichia coli* at 1.4 Å resolution. *J. Mol. Biol.* **247**, 947–962.
11. Feng, Y., Sligar, S. G. & Wand, A. J. (1994). Solution structure of apocytochrome b_{562}. *Nature Struct. Biol.* **1**, 30–34.
12. Laidig, K. E. & Daggett, V. (1996). Molecular dynamics simulations of apocytochrome b_{562}—the highly ordered limit of molten globules. *Fold. Des.* **1**, 335–346.
13. Assfalg, M., Banci, L., Bertini, I., Ciofi-Baffoni, S. & Barker, P. D. (2001). (15)N backbone dynamics of ferricytochrome b(562): comparison with the reduced protein and the R98C variant. *Biochemistry*, **40**, 12761–12771.
14. D'Amelio, N., Bonvin, A., Czisch, M., Barker, P. D. & Kaptein, R. (2002). The C terminus of apocytocrome b_{562} undergoes fast motions and slow exchange among ordered conformations resembling the folded state. *Biochemistry*, **41**, 5505–5514.
15. Barker, P. D., Nerou, E. P., Freund, S. M. V. & Fearnley, I. M. (1995). Conversion of cytochrome b_{562} to *c*-type cytochromes. *Biochemistry*, **34**, 15191–15203.
16. Wittung-Stafshede, P., Gray, H. B. & Winkler, J. R. (1997). Rapid formation of a four-helix bundle. Cytochrome *b*(562) folding triggered by electron transfer. *J. Am. Chem. Soc.* **119**, 9562–9563.
17. Wittung-Stafshede, P., Lee, J. C., Gray, H. B. & Winkler, J. R. (1999). Cytochrome b_{562} folding triggered by electron transfer: approaching the speed limit for formation of a four-helix-bundle protein. *Proc. Natl Acad. Sci. USA*, **96**, 6587–6590.
18. Eaton, W. A., Munoz, V., Thompson, P. A., Henry, E. R. & Hofrichter, J. (1998). Kinetics and dynamics of loops, alpha-helices, beta-hairpins, and fast-folding proteins. *Accts Chem. Res.* **31**, 745–753.
19. Hagen, S. J., Hofrichter, J., Szabo, A. & Eaton, W. A. (1996). Diffusion-limited contact formation in unfolded cytochrome *c*: estimating the maximum rate of protein folding. *Proc. Natl Acad. Sci. USA*, **93**, 11615–11617.
20. Thirumalai, D. (1999). Time scales for the formation of the most probable tertiary contacts in proteins with applications to cytochrome *c*. *J. Phys. Chem. B*, **103**, 608–610.
21. Telford, J. R., WittungStafshede, P., Gray, H. B. & Winkler, J. R. (1998). Protein folding triggered by electron transfer. *Accts Chem. Res.* **31**, 755–763.
22. Wittung-Stafshede, P. (1999). Effect of redox state on unfolding energetics of heme proteins. *Biochim. Biophys. Acta*, **1432**, 401–405.
23. Lee, J. C., Gray, H. B. & Winkler, J. R. (2001). Cytochrome c' folding triggered by electron transfer: fast and slow formation of four-helix bundles. *Proc. Natl Acad. Sci. USA*, **98**, 7760–7764.
24. Moore, G. R. & Pettigrew, G. W. (1990). *Cytochromes* c*: Evolutionary, Structural and Physiochemical Aspects*, Springer Series in Molecular Biology, Springer-Verlag, Berlin.
25. Springs, S. L., Bass, S. E. & McLendon, G. L. (2000). Cytochrome b_{562} variants: a library for examining redox potential evolution. *Biochemistry*, **39**, 6075–6082.
26. Fersht, A. R. (1999). *Structure and Mechanism in Protein Science*, W.H. Freeman, New York.
27. Matouschek, A., Kellis, J. T., Jr, Serrano, L., Bycroft, M. & Fersht, A. R. (1990). Transient folding intermediates characterized by protein engineering. *Nature*, **346**, 440–445.
28. Shastry, M. C. & Roder, H. (1998). Evidence for barrier-limited protein folding kinetics on the microsecond time scale. *Nature Struct. Biol.* **5**, 385–392.
29. Shastry, M. C. R., Sauder, J. M. & Roder, H. (1998). Kinetic and structural analysis of submillisecond folding events in cytochrome *c*. *Accts Chem. Res.* **31**, 717–725.
30. White, A. (1959). Effect of pH on fluorescence of tyrosine, tryptophan and related compounds. *Biochem. J.* **71**, 217–220.
31. Arnesano, F., Banci, L., Bertini, I., Ciofi-Banoffi, S., de Lumley Woodyear, T., Johnson, C. M. & Barker, P. D. (2000). Structural consequences of *b*- to *c*-type cytochrome conversion in oxidized *Escherichia coli* cytochrome b_{562}. *Biochemistry*, **39**, 1499–1514.
32. Van Nuland, N. A., Meijberg, W., Warner, J., Forge, V., Scheek, R. M., Robillard, G. T. & Dobson, C. M. (1998). Slow cooperative folding of a small globular protein HPr. *Biochemistry*, **37**, 622–637.
33. Arnesano, F., Banci, L., Bertini, I. & Koulougliotis, D. (1998). Solution structure of oxidized rat microsomal cytochrome *b*5 in the presence of 2 M guanidinium chloride: monitoring the early steps in protein unfolding. *Biochemistry*, **37**, 17082–17092.
34. Arnesano, F., Banci, L., Bertini, I., Koulougliotis, D. & Monti, A. (2000). Monitoring mobility in the early steps of unfolding: the case of oxidized cytochrome *b*(5) in the presence of 2 M guanidinium chloride. *Biochemistry*, **39**, 7117–7130.
35. Mayor, U., Johnson, C. M., Daggett, V. & Fersht, A. R. (2000). Protein folding and unfolding in microseconds to nanoseconds by experiment and simulation. *Proc. Natl Acad. Sci. USA*, **97**, 13518–13522.
36. Barker, P. D., Nerou, E. P., Cheesman, M. R., Thomson, A. J., de Oliveira, P. & Hill, H. A. O. (1996). Bis-methionine ligation to heme iron in mutants of cytochrome b_{562}. 1. Spectroscopic and electrochemical characterisation of the electronic properties. *Biochemistry*, **35**, 13618–13626.
37. Barker, P. D. & Freund, S. M. V. (1996). Bis-methionine ligation to heme iron in mutants of cytochrome b_{562}. 2. Characterization by NMR of heme-ligand interactions. *Biochemistry*, **35**, 13627–13635.
38. Arcovito, A., Gianni, S., Brunori, M., Travaglini-Allocatelli, C. & Bellelli, A. (2001). Fast coordination changes in cytochrome *c* do not necessarily imply folding. *J. Biol. Chem.* **276**, 41073–41078.
39. Robinson, C. R., Liu, Y. F., O'Brien, R., Sligar, S. G. & Sturtevant, J. M. (1998). A differential scanning calorimetric study of the thermal unfolding of apo- and holo-cytochrome b_{562}. *Protein Sci.* **7**, 961–965.
40. Robinson, C. R., Liu, Y. F., Thomson, J. A., Sturtevant, J. M. & Sligar, S. G. (1997). Energetics of heme binding to native and denatured states of cytochrome b_{562}. *Biochemistry*, **36**, 16141–16146.
41. Dinner, A. R. & Karplus, M. (2001). The roles of stability and contact order in determining protein folding rates. *Nature Struct. Biol.* **8**, 21–22.
42. Fersht, A. R. (2000). Transition-state structure as a unifying basis in protein- folding mechanisms:

contact order, chain topology, stability, and the extended nucleus mechanism. *Proc. Natl Acad. Sci. USA*, **97**, 1525–1529.
43. Gill, S. C. & Hippel, P. H. v. (1989). Calculation of protein extinction coefficients from amino acid sequence data. *Anal. Biochem.* **182**, 319–326.
44. Shastry, M. C., Luck, S. D. & Roder, H. (1998). A continuous-flow capillary mixing method to monitor reactions on the microsecond time scale. *Biophys. J.* **74**, 2714–2721.
45. Wider, G., Neri, D., Otting, G. & Wuthrich, K. (1989). A heteronuclear 3-dimensional NMR experiment for measurements of small heteronuclear coupling-constants in biological macromolecules. *J. Magn. Reson.* **85**, 426–431.
46. Vuister, G. W. & Bax, A. (1993). Quantitative *J* correlation—a new approach for measuring homonuclear 3-bond J(H(N)H(alpha) coupling-constants in N-15- enriched proteins. *J. Am. Chem. Soc.* **115**, 7772–7777.
47. Johnson, B. A. & Blevins, R. A. (1994). NMR View–a computer program for the visualization and analysis of NMR data. *J. Biomol. NMR*, **4**, 603–614.
48. Macura, S., Wuthrich, K. & Ernst, R. R. (1982). The relevance of *J*-cross-peaks in two-dimensional NOE experiments of macromolecules. *J. Magn. Reson.* **47**, 351–357.
49. Marion, D. & Wuthrich, K. (1983). Application of phase sensitive two-dimensional correlated spectroscopy (COSY) for measurements of ^{1}H-^{1}H spin-spin coupling constants in proteins. *Biochem. Biophys. Res. Commun.* **113**, 967–974.
50. Farrow, N. A., Zhang, O., Forman-Kay, J. D. & Kay, L. E. (1994). A heteronuclear correlation experiment for simultaneous determination of ^{15}N longitudinal decay and chemical exchange rates of systems in slow equilibrium. *J. Biomol. NMR*, **4**, 727–734.
51. Mulder, F. A., Van Tilborg, P. J., Kaptein, R. & Boelens, R. (1999). Microsecond time scale dynamics in the RXR DNA-binding domain from a combination of spin-echo and off-resonance rotating frame relaxation measurements. *J. Biomol. NMR.* **13**, 275–288.

Edited by F. Schmid

(Received 26 July 2004; received in revised form 8 November 2004; accepted 17 November 2004)